Modifying the adsorption characteristics of water on Ru{0001} with preadsorbed oxygen

M. J. Gladys,[1,4] A. A. El-Zein,[1] A. Mikkelsen,[2] J. N. Anderson,[2] and G. Held[1,3]
[1]*Department of Chemistry, University of Cambridge, Cambridge CB2 1EW, United Kingdom*
[2]*Department of Physics, Lund University, Lund, Box 1118, S-221 00, Lund, Sweden*
[3]*Department of Chemistry, University of Reading, Whiteknights, RG6 6AD, United Kingdom*
[4]*School of Mathematical and Physical Sciences, University of Newcastle, Callaghan, NSW 2308, Australia*
(Received 28 January 2008; revised manuscript received 27 May 2008; published 3 July 2008)

The coadsorption of water and preadsorbed oxygen on Ru{0001) was studied by synchrotron-based high-resolution x-ray photoelectron spectroscopy. A dramatic change was observed in the interaction of water with oxygen between low and high oxygen precoverages. Low oxygen coverages below 0.18 ML induce partial dissociation, which leads to an adsorbed layer of H_2O and OH. Around half the oxygen atoms take part in this reaction. All OH recombines upon heating to 200 K and desorbs together with H_2O. Oxygen coverages between 0.20 and 0.50 ML inhibit dissociation, instead a highly stable intact water species is observed, which desorbs at 220 K. This species is significantly more stable than intact water on the clean surface. The stabilization is most likely due to the formation of hydrogen bonds with neighboring oxygen atoms. For intermediate oxygen coverages around 0.18 ML, the dissociation behavior depends on the preparation conditions, which points toward possible mechanisms and pathways for partial dissociation of water on Ru{0001}.

DOI: 10.1103/PhysRevB.78.035409 PACS number(s): 68.43.Fg, 79.60.Dp, 82.30.Rs, 61.05.cj

I. INTRODUCTION

After more than 25 years of studying water adsorption on Ru{0001},[1–17] there is still an ongoing debate about the exact nature of the system. Feibelman's recent suggestion that the most stable adsorption structure is in fact a partially dissociated hydrogen-bonded network of H_2O and OH (Ref. 7) generated a flurry of interest in the topic with experimental and theoretical studies, claiming both partial dissociation and intact adsorption. It seems to be agreed upon that at low temperatures around 100 K, water adsorbs molecularly intact while H_2O dissociates partially around and above 160 K. The debate continues whether D_2O partially dissociates or not.[10–13] In addition, recent studies have revealed the ease at which water on Ru{0001} can be electron stimulated into partial and complete dissociation on this surface, and thus reach lower energy states than those accessible by thermal stimulation alone.[11,13] All this indicates that the dissociated and intact adsorption states of water on Ru{0001} are very close in energy with similar activation energies for desorption and dissociation,[7,15,16] which is basically due to the competition between intermolecular hydrogen bonds and water-metal bonds of similar strengths. In such systems kinetic effects play an important role and metastable states can have very long lifetimes. The bulk phase diagram of water ice is a prominent example for this type of system.

Relatively small surface modifications, such as the coadsorption of another species, can have dramatic effects in an adsorption system of this type if they shift the energy balance in one direction or change the activation energies. It has been discovered very early on by Doering and Madey[3] that small amounts of oxygen on Ru{0001} can alter the desorption behavior of water significantly, which turns out to be a general feature of the coadsorption of oxygen and water on metal surfaces.[5,8] In view of the debate over partial dissociation of water on Ru{0001}, it is imperative to reevaluate the assumptions made by previous authors who generally assumed that water stays intact when interacting with oxygen.[2–4] Only in a recent infrared spectroscopy study by Clay *et al.*[12] was the possibility of water dissociation pointed out when coadsorbed with low coverages of oxygen. Using temperature-programed desorption (TPD), Doering and Madey found a significant change in the overall shape of the desorption spectra between low and high oxygen coverages with a sharp transition between 0.20 and 0.25 ML O, indicating a change in the interaction of H_2O and O adatoms on the surface. The first conclusive experimental proof that water can indeed dissociate even on the clean Ru{0001} surface came from an x-ray photoelectron spectroscopy (XPS) study by Weissenrieder *et al.*[10] Using the same technique, we recently showed that the different desorption behaviors in the high and low oxygen-coverage regimes are related to a change from dissociative to molecular adsorption of water.[18] In this paper, we concentrate on the chemical interaction between H_2O and O on Ru{0001}, and explore the phase diagram of water and oxygen coadsorption for oxygen coverages up to 0.50 ML.

The phase diagram of oxygen on Ru{0001} is well studied.[19–22] Two ordered superstructures were formed under UHV conditions, $p(2\times2)$-O for 0.25 ML and $p(2\times1)$ for 0.50 ML,[23,24] which play a central role in this study.

Following to the adsorption behavior of water, the "results" in Sec III is divided into three parts: Low oxygen coverages induce partial dissociation (Sec. III B) whereas oxygen coverages between 0.25 and 0.50 ML do not allow partial dissociation to occur but lead to the formation of a stable species of intact water at high temperatures between 180 and 220 K (Sec. III A). At intermediate oxygen coverage around 0.18 ML, we find that the dissociation behavior depends on the preparation conditions (Sec. III C). Possible adsorption geometries and mechanisms for partial dissociation of water on Ru{0001} are discussed in Sec IV.

II. EXPERIMENT

The experiments were performed at beamline I311 of MAXLAB in Lund, Sweden and at the SuperESCA beamline of Elettra in Trieste, Italy. A Scienta 200 mm hemispherical analyzer was used at MAX-laboratory and a double pass hemispherical electron energy analyzer with a 96-channel detector at Elettra. In both cases, the detection angle was close to the surface normal. X-ray photoelectron (XP) spectra were taken either at constant temperature or during annealing. For the O 1*s* (Ru 3*d*) spectra, photon energies of 625 eV (400 eV) were used with an overall energy resolution, $\Delta E=0.23(0.12)$ eV. The valence-band spectra were recorded with photon energies of 136 eV at an energy resolution of $\Delta E=0.14$ eV. No forward focusing or diffraction effects were observed using these kinetic energies. Temperature-programed XP spectra (TPXPS) were collected by recording continuously fast XP spectra of 15 s duration each while the sample was annealed with a heating rate of 0.1 K/s (1.5 K/spectrum). All experimental XP spectra were fitted with Doniac-Sunic-type line shapes.[25] Unless otherwise stated the accuracy of the peak areas was approximately 0.01 ML. When fitting the Ru 3*d* core-level spectra the number and start positions of peaks were based on physical considerations outlined in previous papers.[22]

The O *K*-edge near-edge x-ray-absorption fine structure (NEXAFS) data shown here were recorded using the hemispherical analyzer at MAX-laboratory to detect the O KLL Auger electrons in the kinetic-energy window (508–515 eV) (pass energy 200 eV). The incoming x-ray beam was either normal to the surface or at grazing incidence (70° off normal), i.e., with the field vector parallel to the surface or tilted by 70° out of the surface plane, respectively. In all cases, O 1*s* XP spectra were recorded before and after collecting the NEXAFS data in order to check for beam-induced changes. No significant changes were observed for the NEXAFS data shown in this paper.

The Ru crystal used for these experiments was oriented within 0.1° to minimize the step density on the surface. The crystal was cleaned in vacuum by cycles of sputtering with 3 keV Argon ions and annealing to 1500 K, followed by oxygen treatment (10^{-7} mbar) and annealing to 1400 K in UHV. Previous studies have shown that surface impurities of the order of a few percent can have a significant effect on the behavior of water on Ru surfaces;[3,12] therefore we have ensured that the surface was clean to levels below the XPS detection limits of oxygen and carbon (<1%) before the start of each experiment. Two different preparation procedures were used to prepare oxygen layers. "As-dosed" oxygen, which pertains to the majority of the experiments, refers to dosing oxygen at 400 K to the required coverage. "Annealed" oxygen layers were prepared by dosing oxygen at 400 K for 300 s at 2×10^{-8} mbar, which leads to the formation of the $p(2\times1)$-O overlayer, followed by annealing to 1100 K for several times until the desired oxygen concentration is achieved.

All oxygen coverages were determined by comparing the O 1*s* XP intensity with that of the $p(2\times1)$ oxygen overlayer. This structure was verified by low-energy electron diffraction (LEED) and good agreement was found with the Ru $3d_{5/2}$ core-level spectra reported by Lizzit *et al.*[22] Fluctuations in the O 1*s* peak intensity were less than 5% for different preparations. Water was dosed at pressures typically around 2×10^{-9} mbar either by back filling the UHV chamber or through a multichannel capillary array doser positioned in line with the sample at a distance of about 4 cm. The amount of water dosed was calibrated via direct comparison of the integrated O 1*s* intensity with that of the $p(2\times1)$-O overlayer.

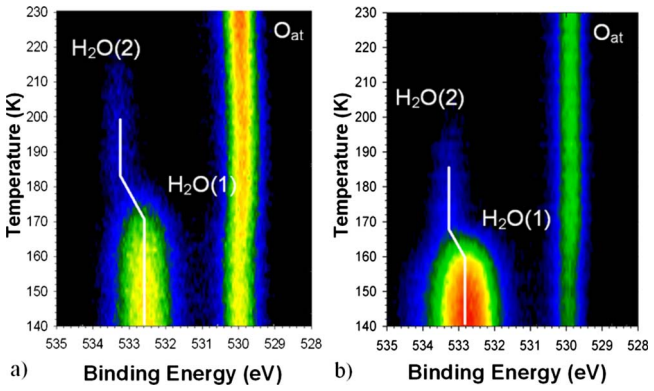

FIG. 1. (Color online) Temperature-programed O 1*s* XPS scans ($h\nu=625$ eV) for (a) 0.75 ML water desorbing from $p(2\times1)$-O and (b) 1.0 ML water desorbing from $p(2\times2)$-O/Ru{0001} surfaces. The water was dosed at 140 K at 2×10^{-9} mbar for 100 s. The sample was annealed at a rate of 0.1 K/s while O 1*s* scans were taken (1.5 K/spectrum).

As discussed earlier, electron stimulated partial and complete dissociation of water is a major problem when using electron-based techniques such as LEED or XPS.[10,11,13] Particular attention was therefore paid to such effects and care was taken to minimize the electron load of the adsorbed layer with single XPS scans equivalent to only 0.01 secondary electrons per molecule, as measured through the sample current. Extensive irradiation of water adsorbed at 140 K on the $p(2\times1)$ and $p(2\times2)$ oxygen surfaces up to 1 electron/molecule showed no changes in the O 1*s* spectra. The absence of any electronic induced effects is opposite to the behavior of the low-temperature water layer on clean Ru{0001}, where even 0.01 electrons/molecule cause the formation of significant amounts of OH.[11,13]

III. RESULTS

This section is divided into three parts: (1) high oxygen coverages, $0.25\ \text{ML}<\theta_o<0.50$ ML, which completely prohibit partial dissociation of water; (2) low oxygen coverages, <0.18 ML, which allow partial dissociation of water; and (3) intermediate coverages, around 0.18 ML, which show a transition from partial dissociation to intact adsorption.

A. High oxygen coverage ≥0.25 ML

A comparison of typical TPXPS plots for water desorption from the $p(2\times1)$-O ($\theta_o=0.50$ ML) and $p(2\times2)$-O ($\theta_o=0.25$ ML) terminated Ru{0001} surfaces is shown in Fig. 1. In both cases water was adsorbed at 140 K and 2

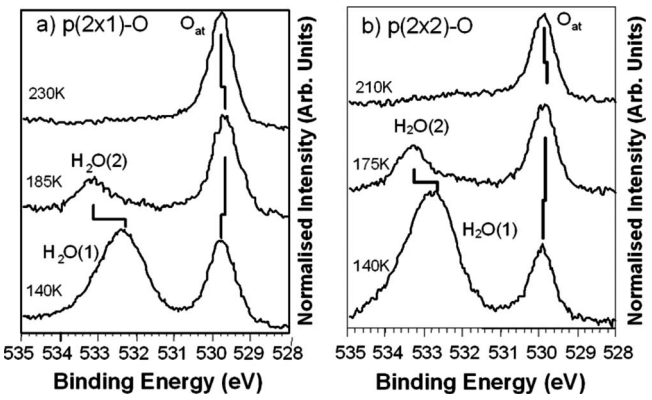

FIG. 2. Individual XP scans from Fig. 1: ($h\nu$=625 eV) (a) 0.75 ML H_2O on $p(2\times1)$-O and (b) 1.0 ML H_2O on (2×2)-O surfaces. At 140 K, both surfaces show the H_2O (1) species of water while at 185/175 K, a second water species [$H_2O(2)$] is present; at 230/210 K only atomic oxygen (O_{at}) is observed.

$\times10^{-9}$ mbar, followed by annealing at a rate of 0.1 K/s (1.5 K/spectrum). Individual scans for temperatures of 140, 185, and 230 K are shown in Fig. 2. Water desorption from the $p(2\times1)$-O adlayer has been described in detail in an earlier publication;[18] it was found that dissociation is suppressed as indicated by the absence of a OH peak around 531 eV. Between 170 and 180 K, most of the water desorbs and the binding energy of the H_2O signal changes from 532.6 [H_2O (1)] to 533.2 eV [H_2O (2)], which is close to that of multilayer ice. Water adsorbed on the $p(2\times2)$-O surface (0.25 ML) behaves very similarly; however there are small differences. After adsorption at 140 K, there is a slightly higher coverage of H_2O, approximately 0.82 ML, as opposed to 0.70 ML on the $p(2\times1)$-O surface. On the $p(2\times2)$-O surface, the water peak at 140 K is centered at 532.8 eV and has a full width at half maximum (FWHM) of approximately 3.6 eV, indicating the presence of both species, H_2O (1) and H_2O (2), already at this temperature. On the $p(2\times1)$-O surface, however, the water feature is centered at 532.6 eV with a significantly narrower FWHM of 2.8 eV. The main desorption peak and the transition to the pure H_2O (2) feature [binding energy (BE) 533.3 eV] occur at slightly lower temperature than on the $p(2\times1)$-O surface around 165 K. The atomic oxygen (O_{at}) signal broadens between 160 and 200 K when the H_2O (2) peak is observed with a change in the FWHM of about 30% for the $p(2\times2)$-O and 10% for the $p(2\times1)$-O surface. At the same time a small shift of −0.10 eV is observed in the BE of O_{at} for 0.25 ML O, whereas the shift is more pronounced with −0.18 eV for 0.50 ML.

The H_2O (2) peaks, after annealing to 175 K/185 K, correspond to a H_2O coverage around 0.12 ML for both oxygen coverages. On saturating the $p(2\times1)$-O surface at 185 K with water at pressures higher than 2×10^{-7} mbar, higher coverages of the H_2O (2) species, up to 0.23 ML, could be achieved, which indicates an activated adsorption process. Figure 3 shows the O 1*s* spectra before and after the adsorption of 20 L water (100 s at 2×10^{-7} mbar) onto the $p(2\times1)$-O surface at 185 K. There is also a clear difference between this spectrum and that shown in Fig. 2(a) with respect to the O_{at} feature. In Fig. 2(a), a single peak was observed with a FWHM up to 10% larger than for the clean oxygen terminated surface. In Fig. 3, however, this feature is significantly broadened and clearly consists of two peaks, O_{at} (1) and O_{at} (2), with BEs of 529.80 and 529.41 eV, respectively. O_{at} (1) has almost the same binding energy as without water. The additional O_{at} (2) feature contributes to approximately 0.16 ML of oxygen, i.e., a third of the total O_{at} signal. Because the two peaks are so close in BE, there is a large error (approximately 0.02 ML) associated with the relative intensities of O_{at} (1) and O_{at} (2). Equal amounts of H_2O (2) and O_{at} (2) would still be in accordance with our data. Dosing the same amount of water below 155 K, and annealing to 185–190 K only produces about half of the H_2O (2) coverage obtainable through dosing at higher temperatures and pressures. This is the reason why we only reported the lower coverage in our previous study.[18]

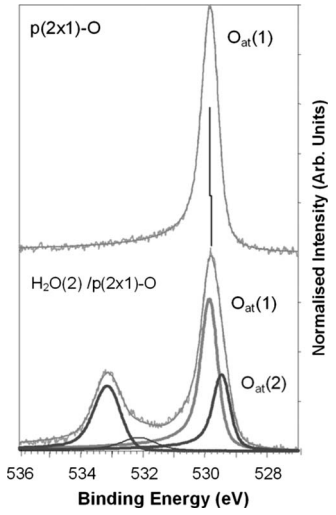

FIG. 3. O 1*s* spectra ($h\nu$=625 eV) of $p(2\times1)$ O on Ru{0001} (top) before and (bottom) after the adsorption of water at 185 K. See text for details.

Each individual XP scan of the TPXPS data sets shown in Fig. 1 was fitted with three peaks, (H_2O (1), H_2O (2), and O_{at}). The integrated intensities of each peak were converted into coverage units as described earlier, and are shown as a function of temperature in the upper part of Figs. 4(a) and 4(b). The derivatives of the H_2O XPS peak areas vs temperature, shown in the lower parts of Fig. 4, are approximately proportional to $d\theta(H_2O)/dT$ (ignoring photoelectron diffraction effects) and can, therefore, be compared directly with TPD spectra in Ref. 3 for the same O precoverages. The peak at 170 K in the derivative of the H_2O (1) signal for the $p(2\times1)$-O precovered surface corresponds to the first desorption peak at 190 K in Ref. 3. The difference between the TPXPS and TPD peak temperatures is due to the different heating rates (0.1 K/s in TPXPS vs 8 K/s in TPD). Very similar shifts have been observed for different heating rates in water desorption from the clean Ru{0001} surface.[13] For the $p(2\times2)$-O surface, both Redhead (assuming first-order desorption kinetics) and leading edge analysis, lead to an activation energy for desorption of 0.53 ± 0.04 eV. The derivative of the H_2O (2) signal has a broad peak between 190

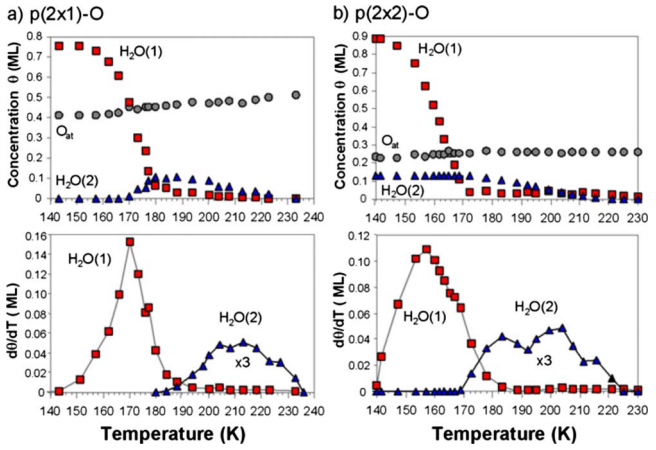

FIG. 4. (Color online) (Top) Adlayer coverage vs sample temperature and (bottom) its derivative, $d\theta/dT$, vs temperature for approximately 1 ML of water adsorbed at 140 K on the (a) $p(2\times1)$-O/Ru{0001} and (b) $p(2\times2)$-O/Ru{0001} surfaces. The H_2O (2) signal (triangles) is multiplied by three in the derivative plot.

and 230 K, which corresponds to the second TPD peak around 235 K in Ref. 3. Using the same analysis as before yields an activation energy of 0.61 ± 0.05 eV. These values compare well with those determined in the same way for water desorption on the $p(2\times1)$-O surface with values of 0.52 and 0.64 eV for H_2O (1) and H_2O (2), respectively.[18] In addition, the activation energy for H_2O (2) on the $p(2\times2)$-O compares very well to the theoretically derived value (0.59–0.62eV) in Ref. 26 for water coverages between 0.25–0.0625 ML by Ref. 26. However, the activation energy for H_2O (1) cannot be compared as the water coverage in the experiments is much higher than theoretically considered in Ref. 26.

Figures 5(a) and 5(b) show series of O 1*s* spectra recorded during the uptake of water at 2×10^{-9} mbar on the $p(2\times1)$-O and $p(2\times2)$-O surfaces at 140 K. It is clear that water is adsorbing intact on the $p(2\times1)$-O surface [Fig. 5(a)] with a single O 1*s* peak at 532.6 eV. The peak has a FWHM of 1.5 eV, typical of single water species on a variety of surfaces,[5] which signifies that the H_2O (2) species is not present at this temperature. Contrary to this, the uptake spectra for the $p(2\times2)$-O surface [Fig. 5(b)] clearly show that the H_2O (2) species populates the surface first, up to a coverage of 0.14 ML, and only then is the H_2O (1) peak observed. The H_2O (2) state populated at 140 K has a binding energy approximately 0.05–0.1 eV higher than that observed on the $p(2\times1)$-O surface at 185 K. When water is adsorbed at 85 K on the $p(2\times2)$-O precovered surface, however, only the H_2O (1) species is observed [Fig. 5(c)]. There are also differences between the O 1*s* binding energies of the H_2O (1) feature on these two surfaces. When adsorbed at 140 K, the BE of the H_2O (1) peak on the $p(2\times1)$-O surface is consistently around 532.2 eV while on the $p(2\times2)$-O surface the feature has a higher BE, 532.6 eV. For adsorption at 85 K, however, the BE is also 532.2 eV on the $p(2\times2)$-O surface. This may be an indication that the H_2O (1) molecules are adsorb in a different orientation when H_2O (2) molecules are present at the surface.

In order to investigate the interaction of water with the Ru surface atoms, Ru $3d_{5/2}$ spectra were recorded for both the $p(2\times1)$ and the $p(2\times2)$ oxygen terminated surfaces before and after water adsorption at 140 and 185 K. In contrast to the O 1*s* core levels, the intensities of the Ru 3*d* core levels cannot be used quantitatively due to stronger electron-diffraction effects. The changes in binding energy, however, are a good means of investigating the interaction of surface Ru atoms with overlayer species. The magnitude of the shift is generally related to the coordination of the probed atom and, the hybridization between the valence orbitals of the probed and surrounding atoms.[22,27]

The spectrum for the $p(2\times1)$-O surface [Fig. 6(a)] is identical to the one reported earlier[22] with surface states assigned to Ru atoms in contact with one [S1(1O)] and two [S1(2O)] oxygen atoms. The BEs of the Ru $3d_{5/2}$ levels for H_2O dosed at 140 K and annealed to 185 K on the $p(2\times1)$-O surface do not change significantly, which suggests that little direct interaction occurs between the water molecules and the Ru surface atoms. This may imply hydrogen

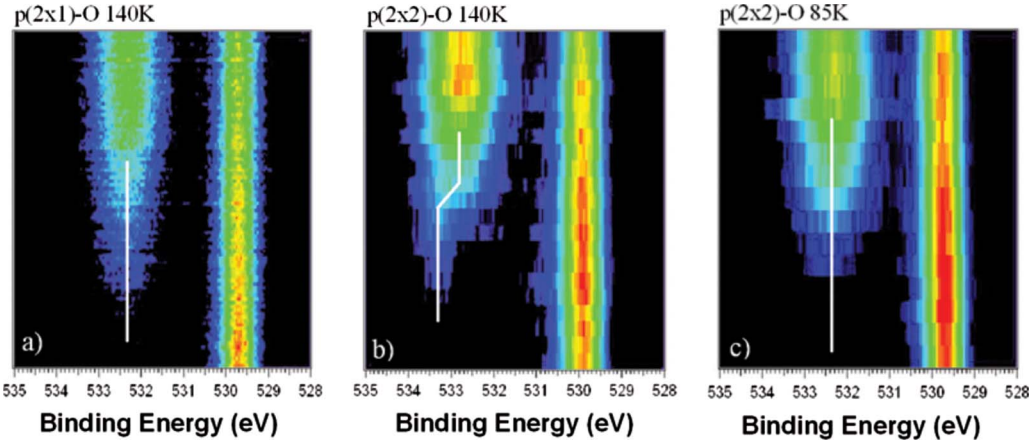

FIG. 5. (Color online) Time-resolved O 1*s* spectra ($h\nu=625$ eV) recorded during dosing of H_2O on (a) $p(2\times1)$-O surface at 140 K with no H_2O (2) species observed. (b) $p(2\times2)$-O at 140 K in which the H_2O (2) species populates the surface first. (c) $p(2\times2)$-O at 85 K with no H_2O (2) species observed. Water pressure$=1.5\times10^{-9}$ mbar for (a), and 4×10^{-9} mbar for (b) and (c). Total dosing time$=900$ s for (a), and 300 s for (b) and (c).

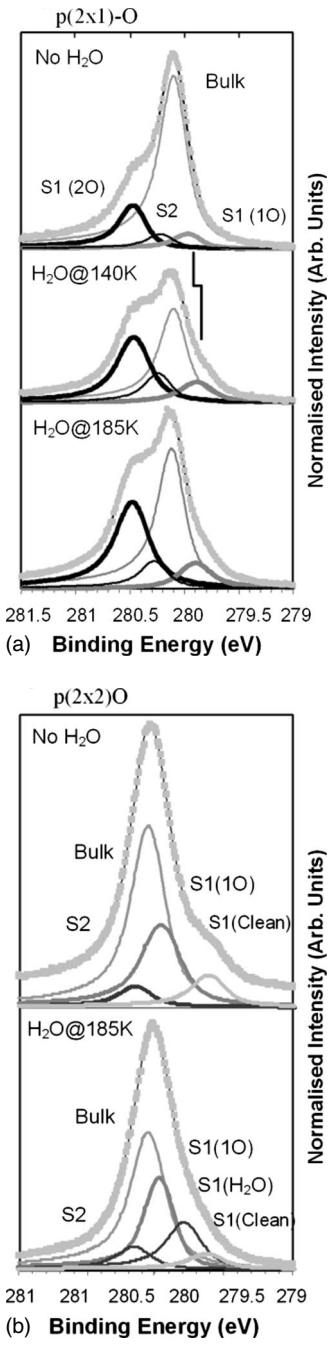

FIG. 6. Ru $3d_{5/2}$ core-level spectra ($h\nu$=400 eV) for (a) $p(2\times1)$-O and (b) $p(2\times2)$-O terminated surfaces of Ru{0001} before and after dosing approximately 0.8 ML water at 140 K. The H_2O(185 K) spectra were taken after dosing water at 140 K and annealing to 185 K.

bonding to the oxygen adatoms instead of direct interaction through the water lone-pair orbitals. Hydrogen bonding to the surface Ru atoms would also not induce a significant change.[10] The S1(1O) peak shifts by −0.05 eV to slightly lower binding energies (279.85 eV), which indicates these atoms are affected to some extent by the presence of water, whereas the S1(2O) peak does not change.

The Ru $3d_{5/2}$ core levels for the $p(2\times2)$-O/Ru{0001} surface before and after water adsorption, and annealing to

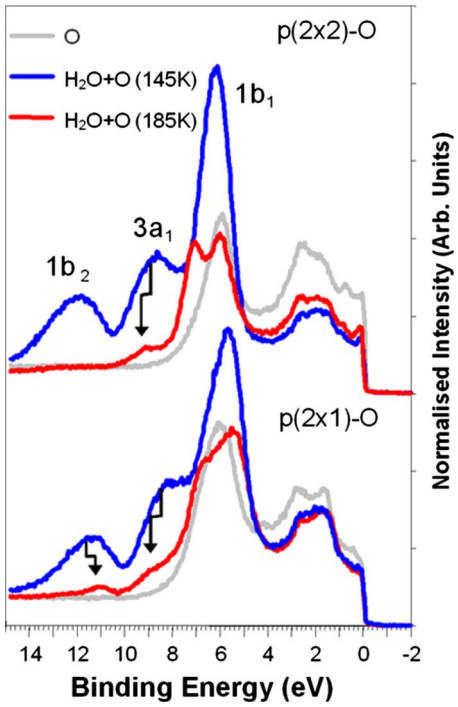

FIG. 7. (Color online) Valence band spectra ($h\nu$=136 eV) for (bottom) $p(2\times1)$-O and (top) $p(2\times2)$-O terminated surfaces of Ru{0001} before and after dosing approximately 0.8 ML water at 145 K. The H_2O+O(185 K) spectra were taken after dosing water at 145 K and annealing to 185 K. See text for details.

185 K are shown in Fig. 6(b). The Ru $3d_{5/2}$ levels after water adsorption at 140 K [H_2O (1) and H_2O (2)] are very similar to those after annealing to 185 K [only H_2O (2)]; they do not seem to be affected by the presence of the H_2O (1) species. The uncovered $p(2\times2)$-O surface has three distinct surface peaks surrounding the bulk peak located at 280.1 eV. The second layer (S2) peak at the high BE side of the bulk feature is at a similar position as for the clean surface in accordance with Lizzit *et al.*[22] On the low BE side there are two surface core-level peaks: S1(1O) at 279.94 eV, which is assigned to Ru surface atoms in contact with one oxygen atom, and S1(Clean), due to the Ru surface atoms that are not interacting directly with an oxygen atom. S1(Clean) has a slightly lower binding energy (279.62 eV) than that of clean Ru surface (279.70 eV), which suggests some next-nearest-neighbor interaction or knock-on effects from Ru atoms in direct contact with oxygen adatoms. In the Ru$3d_{5/2}$ spectrum for the H_2O (2)-covered $p(2\times2)$-O surface, a new surface peak S1(H_2O) with BE 279.84 eV is needed to achieve a good fit to the data, which is shifted by almost 0.2 eV with respect to S1(Clean). S1(H_2O) is assigned to Ru atoms in direct contact with H_2O (2). The S1(1O) Ru surface peak shows only a small shift of 0.05 eV. Combining the information from the Ru core level shifts with that of the O 1*s* data, it appears that the bonding of the H_2O (2) on the $p(2\times2)$-O and the $p(2\times1)$-O surfaces is very similar.

Figure 7 shows the valence-band spectra before and after water adsorption on $p(2\times1)$-O and $p(2\times2)$-O overlayers for 145 and 185 K. For water adsorbed at 145 K, three molecular bands are clearly observed, which are assigned to the

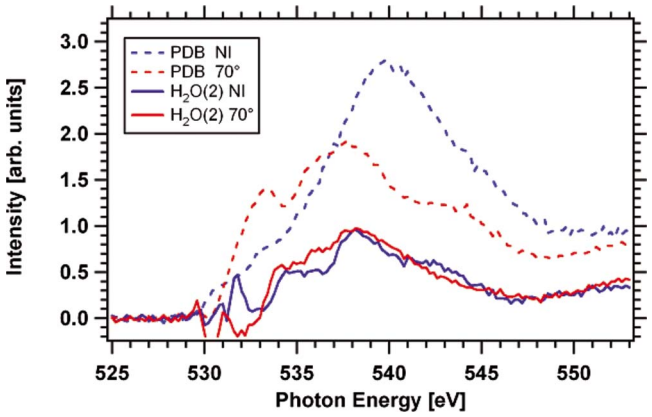

FIG. 8. (Color online) Comparison of O *K*-edge NEXAFS spectra for the PDB of water on clean Ru{0001} (dashed lines) dosed at 165 K and the H_2O (2) species (0.21 ML) on the $p(2\times1)$-O terminated surface dosed at 185 K (solid lines, signal of atomic oxygen subtracted). The dark (blue) and light (red) scans originate from NI and 70° off-normal (70°) incidence geometries.

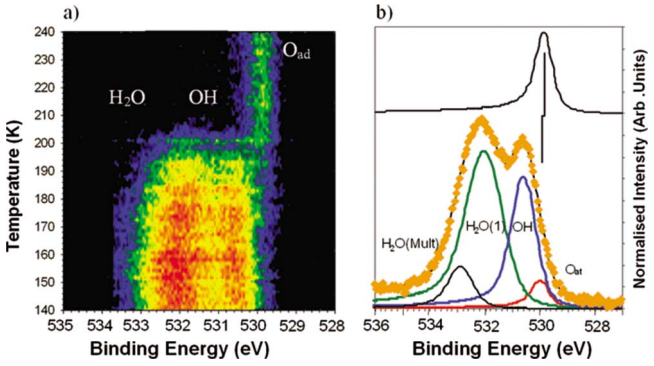

FIG. 9. (Color online) (a) Temperature-programed O 1*s* XPS scans ($h\nu$=625 eV) for 0.57 ML water desorbing from 0.11 ML O/Ru{0001}; the sample was annealed at a rate of 0.1 K/s while O 1*s* scans were taken (1.5 K/spectrum). (b) Single O 1*s* spectrum of water adsorbed at 140 K. The majority of the surface consists of approximately half a dissociated bilayer, which is stable up to about 190 K.

occupied molecular orbitals $1b_2$, $3a_1$, and $1b_1$.[5] $1b_2$ and $3a_1$ are involved in the bonding between the oxygen and hydrogen atoms; their presence indicates that the water is predominately intact on the surface. When water is adsorbed at 185 K, where only the H_2O (2) feature is observed, the $1b_1$ and $3a_1$ orbitals are shifted by about +1 eV in BE, which correlates well to the observed core-level shift observed for the O 1*s* peak for H_2O (2). The $1b_2$ orbital shows a downward shift in BE and a very low excitation cross section that depends on the detection angle and is, therefore, most likely a matrix-element effect related to the geometry of the experiment and orbital symmetry.

In order to gather more information about the bond orientation, oxygen *K*-edge NEXAFS data were recorded for the H_2O (2) species adsorbed onto the $p(2\times1)$-O overlayer at 185 K (1×10^{-7} mbar and 300 s) and the partial dissociated bilayer (PDB) on the clean surface (adsorbed at 165 K) for comparison. Figure 8 shows data for the incoming x-ray beam normal (NI) to the surface and for grazing incidence (70° off normal), i.e., with the electrical field vector parallel to the surface and tilted by 70° out of the surface plane. The H_2O (2) data in Fig. 8 are difference spectra of the $p(2\times1)$-O overlayer with and without water adsorbed; the features between 530 and 532 eV are due to incomplete cancellation of the signal originating from atomic oxygen. These spectra are in good qualitative agreement with spectra published for ice on Ru{0001} (Ref. 28) or intact water on Pt{111} (Ref. 29). The fact that there is very little difference between the two field vector polarizations indicates that the molecular plane is not parallel to either of the field vectors, in particular not parallel to the surface. This is in contrast to the PDB spectra, which show a large anisotropy, compatible with the adsorption geometry of molecules parallel to the surface, as suggested by Feibelman.[7] From these spectra we conclude that the H_2O (2) water molecules on the $p(2\times1)$-O precovered surface are tilted with respect to the surface plane.

B. Low coverages $\theta_o < 0.18$ ML

Predosing 0.11 ML of oxygen onto Ru{0001} leads to TPXPS plots for water desorption, as shown in Fig. 9(a). Figure 9(b) shows individual scans including fits of the oxygen-covered surface before and after dosing water at 140 K. It is clear from this figure that partial dissociation takes place already at this temperature with O 1*s* peaks at BE 532.05 and 530.60 eV assigned to H_2O and OH, respectively. The H_2O-to-OH ratio and their binding energies show a similar temperature dependence as that observed previously for the PDB on the clean Ru{0001} surface.[10] In particular, the OH and H_2O signals disappear together with a constant ratio of 3:5 at all times; the partially dissociated layer is completely desorbed after annealing to 210 K. The integrated peak intensities of the H_2O and OH signals correspond to an (H_2O+OH) coverage of 0.6 ML. The small peak at 533.2 eV indicates a small amount of multilayer water at 140 K. After the adsorption of water, we observe a large reduction of 70% in the integrated O_{at} peak intensity (at 530 eV). With a photon energy of 625 eV, the photoelectrons have a kinetic energy of 95 eV and an inelastic mean-free path of 12 Å through water/ice.[30] This causes a maximum decrease in the O_{at} signal of 20% when attenuated by a single layer. The fitted O_{at} peak after water adsorption, however, has around 70% less intensity compared to the pure oxygen layer, which indicates that at least 60% of the oxygen atoms have reacted with H_2O to form OH. There is a large shift of +0.1 eV in the binding energy of O_{at}, indicating that there is substantial interaction between the water bilayer with the remaining 0.04 ML of oxygen. The OH and H_2O peaks are only marginally shifted (~−0.04 eV) with respect to the PDB on the clean surface.

Figure 10(a) shows the integrated peak intensities of the H_2O, OH, and O_{at} signals [obtained by fitting the individual XP scans of Fig. 9(a)] as a function of temperature. The corresponding derivative of the total amount of dissociated and intact water on the surface (two H_2O peaks plus OH peak) is shown in Fig. 10(b) as a function of temperature.

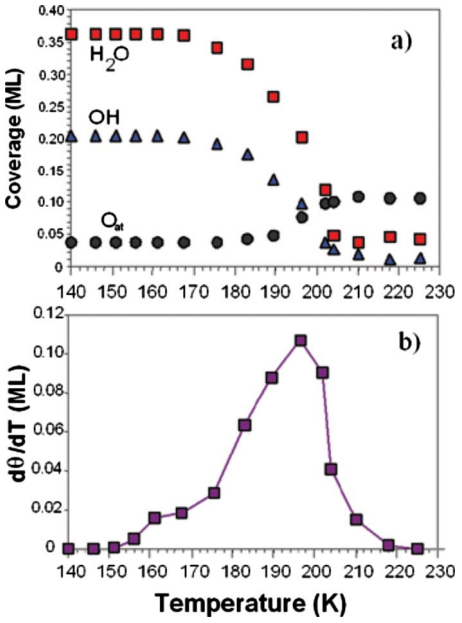

FIG. 10. (Color online) (a) Coverage dependence of the O 1*s* XPS peaks from Fig. 9. (b) Derivative, $d\theta/dT$, of the combined (H_2O+OH) signal vs temperature.

This plot has one maximum between 195 and 200 K, which signifies the simultaneous desorption of intact water and recombination of OH+H. After annealing to 230 K, the oxygen adatom concentration returns to almost the same value (to within 0.005 ML) as before water adsorption.

A comparison of Ru $3d_{5/2}$ spectra for the Ru{0001} surface covered with 0.1 (top) and H_2O+0.1 ML O (bottom) is shown in Fig. 11. The adsorption of oxygen causes an extra peak S1(1O) at BE 279.95 eV to grow, which is assigned to Ru atoms sharing a bond with a single oxygen atom. For the oxygen coverage of 0.11 ML, about 70% of the Ru atoms are not in direct contact with any oxygen atom. These contribute

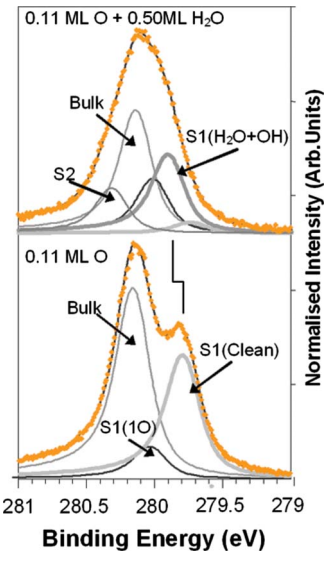

FIG. 11. (Color online) Ru $3d_{5/2}$ core-level spectra ($h\nu$ =400 eV) for 0.55 ML water adsorbed on 0.11 ML O/Ru{0001} at 140 K.

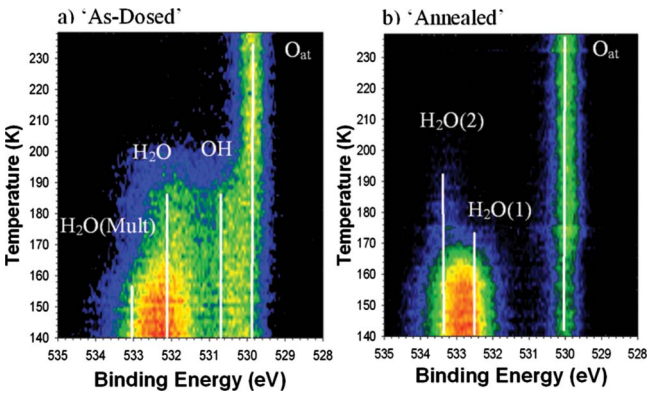

FIG. 12. (Color online) Temperature-programed O 1*s* XPS scans ($h\nu$=625 eV) for (a) 0.60 ML water adsorbed on 0.18 ML O/Ru as dosed at 140 K and (b) 0.70 ML water adsorbed on 0.18 ML O/Ru annealed at 140 K. The sample was annealed at a rate of 0.1 K/s while O 1*s* scans were taken (1.5 K/spectrum). See text for further details.

to the S1(Clean) peak at BE 279.69 eV. The Ru $3d_{5/2}$ spectrum after water adsorption at 140 K is shown at the bottom of Fig. 11. Contact with the water and hydroxyl species in the partially dissociated layer clearly changes the core levels of the surface atoms, and leads to a Ru $3d_{5/2}$ spectrum similar to that obtained for the PDB adsorbed on the clean surface at 165 K.[10]

Since the majority of the Ru surface atoms are not in direct contact with oxygen, it is perhaps not surprising that XP spectra are very similar to the clean surface. However the barrier for dissociation is significantly reduced. On the clean surface, fast dissociation is only observed above 150 K, whereas on the O-covered surface, dissociation readily occurs already at 140 K within the saturated surface. Another difference is the fact that oxygen reacts with water to form OH, thus removing atomic hydrogen from the surface, which must be accommodated otherwise if dissociation takes place on the clean surface.

C. Intermediate region θ_o=0.18 ML

The transition from partial dissociation at lower oxygen coverages to intact H_2O adsorption at higher coverages takes place around 0.20 ML O. In this coverage range the chemical composition of the adsorbed water layer depends critically on the way how the preadsorbed oxygen layer has been prepared. Two layers, each consisting of 0.18 (±0.01) ML O were prepared as dosed (oxygen dosed at 400 K) and annealed (higher coverage of oxygen annealed to 1100 K to reduce down to 0.18 ML), respectively. The TPXPS scans after water adsorption at 140 K in Fig. 12 show big differences between the two surfaces with respect to the chemical composition of the adsorbed layer and the desorption behavior. The latter is even clearer from the $d\Theta_{H_2O}/dT$ spectra shown in Fig. 13. The spectra for the as-dosed prepared surface indicate the formation of a partially dissociated water layer. Figure 14 shows single spectra after adsorption at 140 K on both surfaces. The spectrum for the as-dosed preparation in the bottom part of Fig. 14 contains peaks assigned to

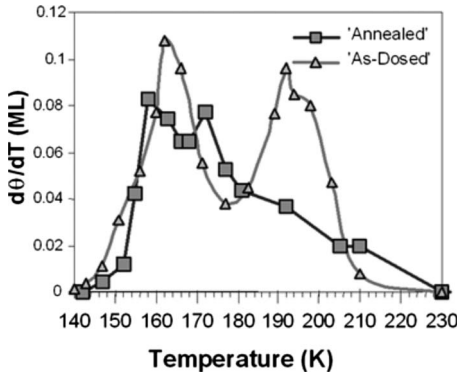

FIG. 13. Derivatives, $d\theta/dT$, of the combined (H_2O+OH) signals vs temperature after water adsorption (0.60 ML) on Ru{0001} covered with 0.18 ML O as dosed and annealed. The as-dosed signal comprises the sum of H_2O (multi), H_2O, and OH peak areas. The annealed signal comprises the sum of H_2O (1) and H_2O (2) peak areas of fits to the TPXPS spectra in Fig. 12.

OH and H_2O, as well as traces of atomic oxygen (O_{at}) and ice [H_2O (multi)]. The annealed surface does not induce dissociation. The spectrum in the top part of Fig. 14 is indicative of molecular adsorption of both the H_2O (1) state (at 532.5 eV) and the H_2O (2) state (at 533.2 eV). This composition is observed between 140 and 170 K. At 170 K the H_2O (1) feature desorbs, leaving only the H_2O (2) species on the surface. This peak is stable up to 190 K and is similar to the feature observed for higher oxygen coverages between 170 and 230 K (see Sec. III A). The main desorption for the H_2O (2) species does, however, occur at a lower temperature than on the $p(2\times2)$-O and $p(2\times1)$-O surfaces; only traces are observed up to 210 K (cf. Fig. 13). The O_{at} peak shifts in the same direction as the $p(2\times2)$-O and $p(2\times1)$-O surfaces but only by −0.05 eV, compared to −0.10 eV and −0.18 eV, respectively, for the higher oxygen coverages.

The individual spectra in the TPXPS series shown in Fig. 12 were fitted with the peaks shown in Fig. 14. Figure 13 shows the derivatives, $-d\Theta_{H_2O}/dT$, of the sums of all fitted

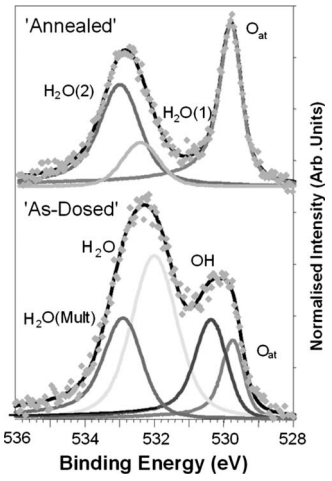

FIG. 14. Fits of the O 1*s* spectra ($h\nu$=625 eV) after water adsorption (2×10^{-9} mbar×300 s) at 140 K onto 0.18 ML O on Ru{0001} as dosed and annealed. See text for details.

peak areas associated with adsorbed water as a function of temperature [i.e., $OH+H_2O+H_2O$ (multi) for as dosed; $H_2O(1)+H_2O(2)$ for annealed]. For the as-dosed preparation, the $d\Theta_{H_2O}/dT$ signal has two distinctive peaks: the first, at 160 K, marks the desorption of the H_2O (multi) species while the second, between 185 and 205 K, is associated with the decrease in the OH signal and the gradual increase in the O_{at} signal due to the disproportionation of OH.

In the uptake sequence of O 1*s* XP spectra (not shown), the 0.18 ML-O as-dosed surface shows growing H_2O and OH peaks from the very beginning, which is indicative of homogenous growth of the partially dissociated layer. On the annealed surface, only the H_2O (2) species is populated initially, as the H_2O (1) species appears subsequently, in the same manner as for the 0.25 ML oxygen-covered surface [cf. Fig. 5(b)].

A comparison between the Ru $3d_{5/2}$ spectra (not shown) for the as-dosed and annealed oxygen terminated surfaces shows small differences. The as-dosed spectrum contains a small clean surface peak S1(Clean) with BE 279.78 eV [surface core level shift (SCLS) of 0.32 eV] while the annealed surface induces a shift of this peak to the lower BE 279.71 eV (SCLS=0.39 eV) similar to the 0.25 ML case.

IV. DISCUSSION AND CONCLUSIONS

The data presented here show that the chemical composition of the water layer adsorbed on Ru{0001} changes substantially as the amount of precovered oxygen increases. Oxygen coverages below 0.18 ML promote the partial dissociation of water above 140 K, which is already observed on the clean surface,[10,12] whereas higher oxygen coverages (above 0.25 ML) inhibit dissociation. In this case, two different intact water species, H_2O (1) and H_2O (2), are observed; the latter of which is significantly more stable than the partially dissociated layer on the clean surface. It is remarkable that partially dissociated, as well as intact, water layers lead to high-temperature desorption peaks around 200 K, which have often been taken as a signature for dissociation/recombination of water.[8] Clearly this is not the case for this system.

For water coadsorption with 0.11 ML O at 140 K, approximately 60% (0.06 ML) of the preadsorbed oxygen is consumed in the reaction with water to produce about 0.20 ML OH_{ad}. The formation of OH on the surface can occur through at least two different pathways. Oxygen could react directly with a water molecule:

$$H_2O_{ad} + O_{at} \rightarrow 2OH_{ad}, \tag{1}$$

or catalyze the partial dissociation:

$$H_2O_{ad} + O_{at} \rightarrow OH_{ad} + H_{at} + O_{at}. \tag{2}$$

According to the coverages determined by XPS, about 60% of the OH in this layer is the result of a direct reaction between water and oxygen [Eq. (1)] whereas the remaining part is produced in a reaction of type (2). Shifts in the H_2O and OH peaks to lower BE, and in the O_{at} peak to higher BE indicate a significant interaction with the remaining oxygen atoms on the surface. The partially dissociated water layer

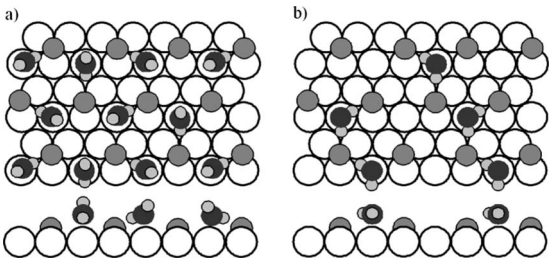

FIG. 15. Possible structures of H_2O (2) on the $p(2\times2)$-O/Ru{0001} surface: (a) (from Ref. 3; 0.25 ML H_2O) the water molecules have one hydrogen bond with a neighboring oxygen adatom with the other hydrogen atom pointing upward, and (b) [from Ref. 26 and Fig. 5(b); 0.125 ML H_2O] the water molecules are parallel to the surface and have two hydrogen bonds with neighboring oxygen atoms.

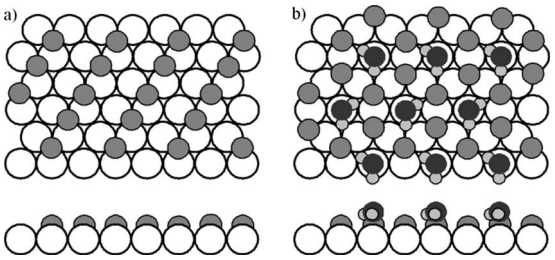

FIG. 16. (a) $p(2\times1)$-O/Ru{0001} overlayer (0.50 ML). (b) Proposed honeycomb structure for water adsorbed onto the 0.50 ML-O/Ru{0001} surface. This structure provides room for the water molecule to interact with both the oxygen and the Ru surface atoms.

forms a network of (H_2O_{ad}+OH_{ad}) base units as found on the clean surface at higher temperatures.[7,10] Wagner and Moylan[31] concluded that molecularly intact water must be present to stabilize the OH formed in the reaction of H_2O and O on Rh{111} because the H_2O and OH disappear simultaneously from the surface. Similar behavior was observed for oxygen and water adsorption on Pt{111} (Refs. 32 and 33) and the clean Ru{0001} surface.[10] The stoichiometry of the resulting [H_2O+OH+O(+H)] layer indicates that both reactions (1) and (2) occur in parallel. Both reactions are reversible, leading to the disproportionation and recombination of OH, and the simultaneous disappearance of H_2O and OH from the surface. After desorption, the exact same amount of O_{at} is present at the surface as before water was adsorbed. In agreement with earlier studies,[2–4,12] we find that about five water molecules are affected per oxygen atom.

For the intermediate coverage of 0.18 ML O (as dosed), only about 45% (0.08 ML) of the preadsorbed oxygen reacts with the coadsorbed water molecules at 140 K to produce 0.17 ML OH, which means that almost all OH is produced by reaction (1). The remaining oxygen atoms are not taking part in the reaction and no BE shift is observed in their XPS signal upon water adsorption.

Oxygen coverages higher than 0.25 ML do not induce any dissociation and the amount of atomic oxygen is not affected by the water layer. Instead, an additional intact water species, H_2O (2), is observed in XPS that has strong surface bonds stable up to 220 K. This desorption temperature is higher than for the partially dissociated layers. Between 0.25 and 0.50 ML, the oxygen overlayer transforms from $p(2\times2)$-O to $p(2\times1)$-O. The H_2O (2) XPS peak has almost identical BEs in both cases, which indicates that the chemical environment for this species is very similar over this entire coverage range. The additional stabilization is most likely due to hydrogen bonding between the water molecules and the oxygen adatoms. Such structures have been proposed previously by Doering and Madey on the basis of their electron stimulated desorption ion distribution (ESDIAD) results.[3] Their model includes one hydrogen bond with an oxygen adatom and one covalent bond with a Ru surface atom (through the lone-pair orbitals) per water molecule, as shown in Fig. 15(a). A similar geometry has been proposed for water adsorption on the $p(2\times2)$-O overlayer on Ni{111}.[34] A covalent bond with the metal substrate would facilitate very efficient screening of the O 1*s* core hole and one would, therefore, expect a lower BE, which is more similar to that of water molecules adsorbed on the clean surface (532.5 eV).[10] The XPS BE found for the H_2O (2) species is, however, much higher, 533.3 eV, which is similar to that of water molecules in ice and, thus, makes a second hydrogen bond, either with Ru or another oxygen atom, more likely. Indeed, very recently a combined discrete Fourier transform (DFT) and scanning tunnel microscopy (STM) study of water on the $p(2\times2)$-O/Ru{0001} surface by Cabrera-Sanfelix *et al.*[26] shows just that. In their favored structure (H_2O coverage 0.125 ML), the water molecule occupies an atop site in the center of the $p(2\times2)$ unit cell and forms extended hydrogen bonds with two neighboring oxygen atoms, which are almost parallel to the surface [Fig. 15(b)]. A comparison with the geometry of the partially dissociated bilayer of H_2O on clean Ru{0001} (Refs. 6 and 7) shows that the molecule in the coadsorption structure is between 0.2 and 0.3 Å further away from the Ru surface atoms, at a distance of 2.37 Å, which is too large for a covalent bond and, hence, explains the difference in XPS binding energies. The parallel hydrogen bonds are not in agreement with the interpretation of our NEXAFS results for the H_2O (2) species on the $p(2\times1)$-O surface; however the tilt angle of the molecular plane may well change when the oxygen coverage is higher. An infrared reflection absorption spectroscopy (IRAS) study by Thiam *et al.*[35] on the adsorption of D_2O on the 1 ML (1×1)-O overlayer on Ru{0001} concluded that the water molecules were in an "oxygen up" configuration with no hydrogen-bonded network between them, which is more in line with our NEXAFS data. All water desorbs below 160 K from this latter surface, which implies that some direct interaction with the Ru substrate is necessary in order to form the stronger bond observed for lower O coverages.

Without support by model calculations or surface crystallography, it is difficult to pin down the exact local geometry of water on the $p(2\times1)$-O surface. Unlike $p(2\times2)$, the $p(2\times1)$-O overlayer [Fig. 16(a)] allows much less room for the water molecules to interact with the surface Ru atoms. Figure 16(b) shows an alternative arrangement for 0.5 ML of oxygen atoms, the so-called "honeycomb" structure, with half the atoms on fcc and the other half on hcp sites. This arrangement would free up a Ru atop adsorption site and allow adsorption geometries similar to that found most favor-

able for the $p(2\times2)$-O surface for all oxygen coverages between 0.25 and 0.50 ML. A tilt of the H-O-H plane at higher O coverage, as indicated by NEXAFS, would also be possible within this structure. Honeycomb structures have been observed for coadsorption of oxygen with CO and NO on Ru{0001}, where a XPS BE shift of 0.35 eV was found between the O_{hcp} and O_{fcc} O 1*s* signals.[36,37] This shift is very similar to that observed here (0.39 eV). A water-induced honeycomb arrangement requires site changes for half the oxygen atoms on the surface, which is kinetically hindered at low temperatures. This would explain why the H_2O (2) species is only observed above 170 K for 0.50 ML O in contrast to the $p(2\times2)$-O layer at 0.25 ML, where it is already found at 140 K (see Figs. 4 and 5). In order to understand the driving forces behind such a rearrangement, *ab initio* calculations will be necessary together with a more definitive characterization of the surface geometry through structural methods such as LEED-IV or STM.

A somewhat puzzling result of our investigation is the dissociation behavior in the intermediate coverage range around 0.18 ML O. The oxygen layer created by dosing at 400 K leads to significant dissociation, whereas the same amount of oxygen deposited by saturating the surface first and then desorbing 64% of the oxygen atoms at 1100 K passivates the surface with respect to water dissociation. If the latter procedure is used to produce layers with lower oxygen coverage, dissociation is observed; for oxygen coverages of 0.25 ML and higher, no dissociation is observed, irrespective of which preparation procedure is used. This indicates that mixed $OH+H_2O$ layers can only form if the local density of oxygen atoms is less than 0.25 ML, presumably due to blocking of adsorption sites for the dissociation products OH and H, both of which need to form a bond with Ru atoms for a stable adsorption configuration.

One possible explanation for the behavior at 0.18 ML O is that the adsorption at 400 K leads to a rather disordered layer of oxygen atoms, as indicated by earlier LEED experiments,[19,23] whereas desorption from the saturated layer at high temperatures leaves behind a surface with large $p(2\times2)$ islands that are not reactive. The shift of 0.05 eV in the S1 binding energy in the Ru $3d_{5/2}$ spectrum between the as dosed and the annealed layer is consistent with this assumption.[22]

An alternative explanation is that the oxygen atoms, when heated to 1100 K, block the active sites for water dissociation, e.g., most likely step edges. It has been shown earlier that oxygen adsorption can lead to modifications of step edges on Ru{0001}.[38] This would imply that dissociation can only occur at a relatively small number of surface sites and that the dissociation products are able to diffuse to their destination sites at around 140 K, which appears plausible if the diffusion step is an exchange of H atoms rather than hopping of the entire OH molecule. Based on our results, we cannot discriminate between these two models; further experiments and/or model calculations will be necessary to clarify this question.

V. SUMMARY

The coadsorption of water and oxygen on Ru{0001} has two very distinct adsorption regimes. For oxygen coverages below 0.18 ML, water can form a partially dissociated bilayer at 140 K. Only part of the oxygen atoms react with water to form OH via the reverse disproportion reaction, the remainder interacts strongly with the water and hydroxyl species as indicated by a shift in the XPS binding energy. Between about 0.20 and 0.50 ML, partial dissociation of water is inhibited at all temperatures and a strongly bound water feature, $H_2O(2)$, is observed at higher temperatures between 170 and 220 K. The XPS binding energy of this species is close to that of hydrogen-bonded water, and the same for $p(2\times1)$ and $p(2\times2)$ oxygen terminated layers, indicating very similar chemical environments. The most likely adsorption complex involves hydrogen bonds with two oxygen atoms and a weak interaction with the Ru surface. At the boundary between the two adsorption regimes, the chemical composition of the water layer depends on the way the oxygen layer was prepared.

ACKNOWLEDGMENTS

This study was supported by EPSRC (through Grant No. GR/S85528/01) and by the European Community—Research Infrastructure Action under the FP6 "Structuring the European Research Area" Programme (through the Integrated Infrastructure Initiative "Integrating Activity on Synchrotron and Free Electron Laser Science," Contract No. R II3-CT-2004–506008). The authors like to express their special thanks to the staff of Maxlab and Elettra, in particular S. Lizzit and L. Paolucci, for assistance during the beamtimes. The authors would also like to thank M. Salmeron for making the manuscript of Ref. 26 available prior to publication.

[1] K. Kretzchmar, J. K. Sass, P. Hofmann, A. Ortega, A. M. Bradshaw, and S. Holloway, Chem. Phys. Lett. **78**, 410 (1981).
[2] K. Kretzchmar, J. K. Sass, A. M. Bradshaw, and S. Holloway, Surf. Sci. **115**, 183 (1982).
[3] D. L. Doering and T. E. Madey, Surf. Sci. **123**, 305 (1982).
[4] P. A. Thiel, F. M. Hoffmann, and W. H. Weinberg, Phys. Rev. Lett. **49**, 501 (1982).
[5] P. A. Thiel and T. E. Madey, Surf. Sci. Rep. **7**, 211 (1987), and references therein.
[6] G. Held and D. Menzel, Surf. Sci. **316**, 92 (1994).
[7] P. J. Feibelman, Science **295**, 99 (2002).
[8] M. A. Henderson, Surf. Sci. Rep. **46**, 1 (2002), and references therein.
[9] S. R. Puisto, J. Lerotholi, G. Held, and D. Menzel, Surf. Rev. Lett. **10**, 487 (2003).
[10] J. Weissenrieder, Anders Mikkelsen, J. N. Andersen, P. J. Feibelman, and G. Held, Phys. Rev. Lett. **93**, 196102 (2004).
[11] K. Andersson, A. Nikitin, L. G. M. Pettersson, A. Nilsson, and

H. Ogasawara, Phys. Rev. Lett. **93**, 196101 (2004).
[12] C. Clay, S. Haq, and A. Hodgson, Chem. Phys. Lett. **388**, 89 (2004).
[13] N. S. Faradshev, K. L. Kostov, P. Feulner, T. E. Madey, and D. Menzel, Chem. Phys. Lett. **415**, 165 (2005).
[14] D. N. Denzler, Ch. Hess, R. Dudek, S. Wagner, Ch. Frischkorn, M. Wolf, and G. Ertl, Chem. Phys. Lett. **376**, 618 (2003).
[15] A. Michaelides, A. Alavi, and D. A. King, J. Am. Chem. Soc. **125**, 2746 (2003).
[16] S. Meng, E. G. Wang, Ch. Frischkorn, M. Wolf, and S. Gao, Chem. Phys. Lett. **402**, 384 (2005).
[17] S. Haq, C. Clay, G. R. Darling, G. Zimbitas, and A. Hodgson, Phys. Rev. B **73**, 115414 (2006).
[18] M. J. Gladys, A. Mikkelsen, J. N. Andersen, and G. Held, Chem. Phys. Lett. **414**, 311 (2005).
[19] H. Pfnür and P. Piercy, Phys. Rev. B **40**, 2515 (1989).
[20] C. Stampfl, S. Schwegmann, H. Over, M. Scheffler, and G. Ertl, Phys. Rev. Lett. **77**, 3371 (1996).
[21] Y. D. Kim, A. P. Seitsonen, and H. Over, Surf. Sci. **465**, 1 (2000).
[22] S. Lizzit, A. Baraldi, A. Groso, K. Reuter, M. V. Ganduglia-Pirovano, C. Stampfl, M. Scheffler, M. Stichler, C. Keller, W. Wurth, and D. Menzel, Phys. Rev. B **63**, 205419 (2001).
[23] M. Lindroos, H. Pfnür, G. Held, and D. Menzel, Surf. Sci. **222**, 451 (1989).
[24] H. Pfnür, G. Held, M. Lindroos, and D. Menzel, Surf. Sci. **220**, 43 (1989).
[25] S. Doniach and M. Sunjic, J. Phys. C **3**, 285 (1970).
[26] P. Cabrera-Sanfelix, D. Sanchez-Portal, A. Mugarza, T. K. Shimizu, M. Salmeron, and A. Arnau, Phys. Rev. B **76**, 205438 (2007).
[27] A. Baraldi, S. Lizzit, G. Comelli, M. Kiskinova, R. Rosei, K. Honkala, and J. K. Nørskov, Phys. Rev. Lett. **93**, 046101 (2004).
[28] D. Coulman, A. Puschmann, U. Höfer, H.-P. Steinrück, W. Wurth, P. Feulner, and D. Menzel, J. Chem. Phys. **93**, 58 (1990).
[29] H. Ogasawara, B. Brena, D. Nordlund, M. Nyberg, A. Pelmenschikov, L. G. M. Pettersson, and A. Nilsson, Phys. Rev. Lett. **89**, 276102 (2002).
[30] A. Akkerman and E. Akkerman, J. Appl. Phys. **86**, 5809 (1999), and references therein.
[31] F. T. Wagner and T. E. Moylan, Surf. Sci. **191**, 121 (1987).
[32] C. Clay, S. Haq, and A. Hodgson, Phys. Rev. Lett. **92**, 046102 (2004).
[33] G. Held, C. Clay, S. D. Barrett, S. Haq, and A. Hodgson, J. Chem. Phys. **123**, 064711 (2005).
[34] M. Nakamura and M. Ito, Phys. Rev. Lett. **94**, 035501 (2005).
[35] M. M. Thiam, T. Kondo, N. Horimoto, H. S. Kato, and M. Kawai, J. Phys. Chem. B **109**, 16024 (2005).
[36] B. Narloch, G. Held, and D. Menzel, Surf. Sci. **317**, 131 (1994).
[37] M. Stichler and D. Menzel, Surf. Sci. **419**, 272 (1999).
[38] G. Held, S. Uremovic, and D. Menzel, Surf. Sci. **331-333**, 1122 (1995).